J Electr Eng Technol.2018; 13(1): 307-314
http://doi.org/10.5370/JEET.2018.13.1.307

ISSN(Print) 1975-0102
ISSN(Online) 2093-7423

Analysis and Optimization of Permanent Magnet Dimensions in Electrodynamic Suspension Systems

Saeed Hasanzadeh†, Hossein Rezaei* and Ehsan Qiyassi**

Abstract – In this paper, analytical modeling of lift and drag forces in permanent magnet electrodynamic suspension systems (PM EDSs) are presented. After studying the impacts of PM dimensions on the permanent magnetic field and developed lift force, it is indicated that there is an optimum PM length in a specified thickness for a maximum lift force. Therefore, the optimum PM length for achieving maximum lift force is obtained. Afterward, an objective design optimization is proposed to increase the lift force and to decrease the material cost of the system by using Genetic Algorithm. The results confirm that the required values of the lift force can be achieved; while, reducing the system material cost. Finite Element Analysis (FEA) and experimental tests are carried out to evaluate the effectiveness of the PM EDS system model and the proposed optimization method. Finally, a number of design guidelines are extracted.

Keywords: Permanent magnet, Suspension systems, Genetic algorithm; Finite element

1. Introduction

Electrodynamic suspension systems are used in various applications such as magnetic bearing, space launchers, rapid transportation, etc. Use of permanent magnet (PM) materials in these systems has attracted increasing attention due to its numerous advantages e.g. no need for super-conductor materials, power sources and active control systems. However, in permanent magnet electrodynamic suspension (PM EDS) systems, the levitation force is low unless there is a considerable motion between the magnets and the conducting sheet. In addition, PM EDS systems usually utilize rare-earth materials such as neodymium permanent magnets. Therefore, decrease in material consumption and its cost is a major issue. Performance analysis and parameter optimization of EDS systems have been the focus of some researches. One way of studying the impacts of PM EDS parameters on its performance, in detail, is by using an analytical model of the system.

The analytical modeling and design of electrodynamic suspension system with halbach arrays are carried out by studying lift and drag forces and approaching the lift to drag ratio and lift to magnet area to the 200:1 and 40 metric tones per square meters, respectively [1]. The mathematical model and static performance analysis of the suspension force, for a magnetic bearing, is presented based on a magnetic equivalent circuit [2]. The restoring axial force and braking torque of the electrodynamic bearing, in terms of magnetic parameters of the bearing, are presented and compared with the experimental results [3]. Optimization of a PM EDS system for decreasing the suspension power loss is done after obtaining the lift force [4]. The analytical model and performance analysis of axial magnetic bearing are developed by a magnetic equivalent circuit model together with the conformal mapping method and Laplace's equation [5]. The multi-objective optimization of the hybrid magnetic bearing shows an improvement of the lift force and a reduction of the required air gap flux density [6]. Although, the analytical model and performance analysis presented for the halbach EDS and magnetic bearings are accurate and general and its optimization is robust, they do not include modeling and optimization of PM EDS systems.

The characteristic analysis of HTS electrodynamic suspension systems is presented [7, 8]. The optimum design of the system superconducting coil and ground conductors are also done. However, the superconducting coil and the ground conductor properties are not considered as continuous variables for the optimization.

Among all the previous works, the performance analysis and optimization of the PM EDS system based on the analytical model is the thing that is concerned rarely. In this paper, the impact of PM dimensions on its magnetic field and developed lift force are investigated. Observations of the magnetic field around PM shows that there is an optimum PM length for achieving a maximum effective sinusoidal magnetic field and a maximum lift force. By choosing length and thickness of the PM as design parameters, an objective function is defined for maximizing lift force; while minimizing material cost as the objective. Then, the optimization is carried out using genetic algorithm (GA) for different objective functions.

† Corresponding Author: Electrical and Computer Engineering, Qom University of Technology, Iran. (hasanzadeh@qut.ac.ir)
* School of Electrical and Computer Engineering, University of Tehran, Iran. (ho.rezaei@alumni.ut.ac.ir)
** University of Massachusetts-Lowell, United States. (ehsan_qiyassi@student.uml.edu)
Received: December 25, 2016; Accepted: October 20, 2017

Finally, an experimental system is built and analytical results are compared with FEM and test results to validate the modelling and the optimization method.

2. PM EDS Model

Fig. 1 depicts the physical model of a PM EDS system. In some applications like suspension system of maglevs, the magnet depth is high with respect to the magnet thickness. Therefore, system can be analyzed by a 2-dimension model as in Fig. 1. The motion of PM with respect to the conducting sheet in the direction of x-axis induces eddy current in the sheet and the interaction between the PM magnetic field and the eddy current sheet develops the lift Fig. 1 depicts the physical model of a PM EDS system. In some applications like suspension system of maglevs, the magnet depth is high with respect to the magnet thickness. Therefore, system can be analyzed by a 2-dimension model as in Fig. 1. The motion of PM with respect to the conducting sheet in the direction of x-axis induces eddy current in the sheet and the interaction between the PM magnetic field and the eddy current sheet develops the lift and drag forces in the directions of y- and x-axis respectively. The lift force elevates the PM to a certain air gap and the drag force opposes the PM movement. The opposing force due to the PM end effect is neglected. Therefore, the end effect is not considered in drag force calculations. It should be noted that the conductor sheet is considered to be thin toward eddy current depth [9].

Variations of PM magnetic field are quasi-sinusoidal with respect to direction of the movement as depicted in Fig. 2.

The fundamental sinusoidal components of horizontal and vertical magnetic fields are also depicted as dotted lines in Fig. 2. Since harmonics of the produced magnetic field do not have any impact on the effective force development; only the fundamental components are taken into the calculations. By assuming a pure sinusoidal magnitude for the magnetic fields, the effective spatial domain of the magnetic field would be 2L.

If a PM develops vertical and horizontal magnetic fields

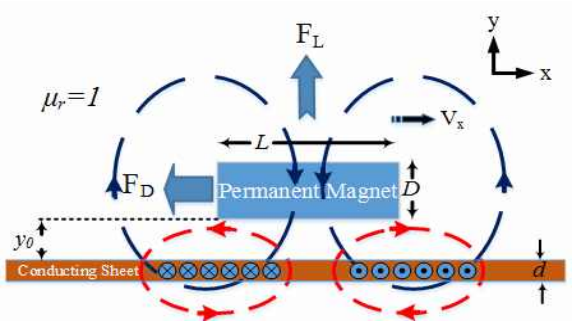

Fig. 1. Physical model of electrodynamic suspension system

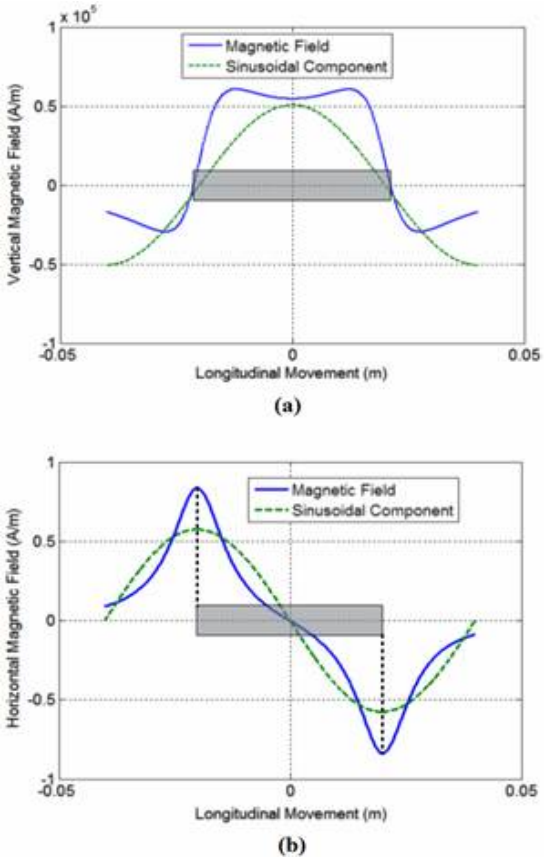

Fig. 2. Permanent magnetic field and its fundamental components. (a) Vertical magnetic field (b) Horizontal magnetic field

which vary sinusoidally with respect to longitudinal movement, the field magnitudes decrease exponentially with respect to distance from PM. Therefore, equations (1) and (2) are given for the calculation of the vertical and horizontal components of magnetic field in y_0 vertical distance from PM [10, 11]:

$$H_x = -h_x \sin\left(\frac{\pi x}{L}\right) e^{-\frac{\pi y_0}{L}} \quad (1)$$

$$H_y = h_y \cos\left(\frac{\pi x}{L}\right) e^{-\frac{\pi y_0}{L}} \quad (2)$$

where h_x and h_y are sinusoidal magnitude of horizontal and vertical magnetic field, L stands for the PM length and y_0 denotes the air gap between PM and conducting sheet. . Since the conductor sheet is considered to be thin toward eddy current depth, magnetic fields and their variations in z direction can be ignored [10]. The developed lift force per unit depth for a sinusoidal permanent magnetic field can be written as [10]:

$$F_L = 2\mu_0 L h_x h_y e^{\frac{-2\pi(y_0+\frac{D}{2})}{L}} \frac{V_x^2}{V_x^2 + w^2}, \quad (3)$$

Also the drag force per unit depth by neglecting the opposing force due to the PM end effect can be expressed as [10]:

$$F_D = 2\mu_0 w L h_y^2 e^{\frac{-2\pi y_0}{L}} \frac{V_x}{V_x^2 + w^2} \quad (4)$$

in which, V_x denotes relative velocity between PM and w can be calculated by:

$$w = \frac{2}{\mu_0 \sigma d}, \quad (5)$$

where, d is the thickness of conductor sheet and σ is its conductivity. According to Fig. 3, the PM can be considered as two current sheets at each PM end. For a PM with linear demagnetization curve, the magnetomotive force may be calculated as:

$$\Theta_{PM} = M_0 D \quad (6)$$

As so, by assuming the sinusoidal magnitude of vertical and horizontal magnetic fields to be equal, h_x and h_y can is obtained as:

$$h_x = H_x(x = -\frac{L}{2}, y = 0) = h_y = H_y(x = 0, y = 0) = H \quad (7)$$

The magnetic field due to current sheet 1 at the point P(r,θ) in Fig. 3 can be written as:

$$H_{1p}(r,\theta) = \frac{\Theta_{PM}}{2\pi r} = \frac{M_0 D}{2\pi r} \quad (8)$$

According to Fig. 3, horizontal and vertical components of H are obtained as:

$$H_{x1p}(r,\theta) = \frac{M_0 D}{2\pi r}\cos(\theta) \quad (9)$$

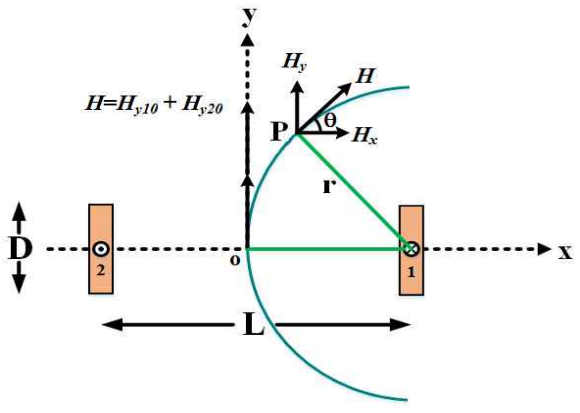

Fig. 3. PM modeling by single current sheet

$$H_{y1p}(r,\theta) = \frac{M_0 D}{2\pi r}\sin(\theta) \quad (10)$$

Vertical magnetic field due to current sheet 1 at the point o(L/2, π/2) is given as:

$$H_{y1O}(\frac{L}{2}, \frac{\pi}{2}) = \frac{M_0 D}{2\pi(\frac{L}{2})} = \frac{M_0 D}{\pi L} \quad (11)$$

Net vertical magnetic field at the point o(L/2, π/2) can be obtained as:

$$H = H_{y1O} + H_{y2O} = \frac{2M_0 D}{\pi L} \quad (12)$$

According to (7) and (12), the sinusoidal magnitudes of horizontal and vertical magnetic fields are expressed by:

$$h_x = h_y = \frac{2M_0 D}{\pi L}. \quad (13)$$

Since H is obtained at the center of PM, y_0 in (1) and (2) is placed by $y_0+D/2$. By substituting (13) into (3) and (4), the lift and drag forces, in terms of system parameters, can be obtained as:

$$F_L = \frac{8\mu_0 (M_0 D)^2}{\pi^2 L} e^{\frac{-2\pi(y_0+\frac{D}{2})}{L}} \frac{V_x^2}{V_x^2 + w^2}, \quad (14)$$

$$F_D = \frac{8w\mu_0 (M_0 D)^2}{\pi^2 L} e^{\frac{-2\pi(y_0+\frac{D}{2})}{L}} \frac{V_x}{V_x^2 + w^2}. \quad (15)$$

3. PM Dimensions Impact on Developed Force

A permanent magnet can be regarded as a magnetic field source with its magnetic flux passing through different air paths reluctances around it. The vertical and horizontal magnetic field distributions of the PM are obtained by 2-D FEM analysis and shown in Figs. 4 and 5. Also the magnetic fields variations with respect to longitudinal movement and their sinusoidal magnitudes are depicted in Figs. 4 and 5 respectively for three different PM lengths of 4, 40 and 120 cm. The figures show that the flux density in both directions tends towards zero in the middle region of the magnet length as the PM length increases; whereas, it remains high at the PM ends. In fact, by increasing the length of the magnet, the vertical and horizontal magnetic fields get closer to the shape of impulse functions and the sinusoidal magnitude of magnetic fields decrease significantly as shown in Figs. 4 and 5. This is due to the increasing reluctance of flux path as the PM length increase. This is only the case

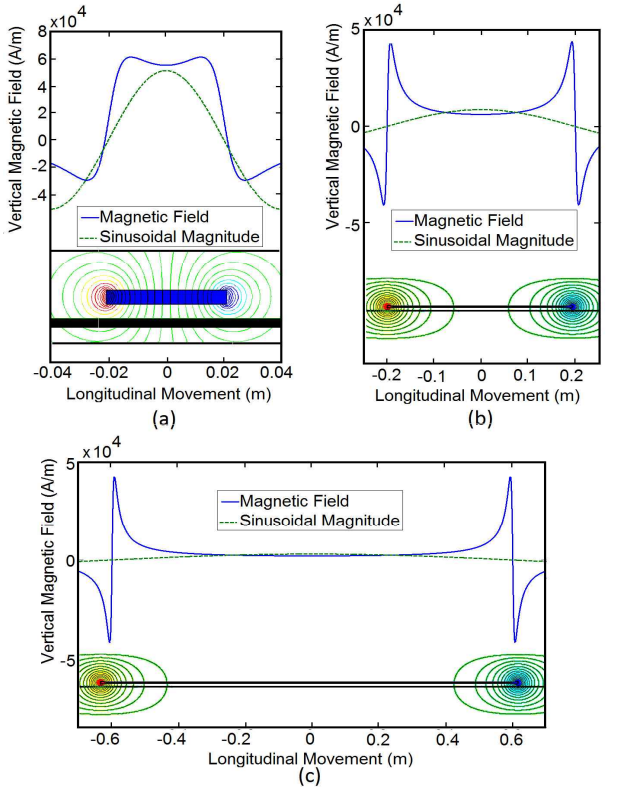

Fig. 4. Vertical magnetic field diagram in different PM lengths (a) L=4cm (b) L=40cm (c) L=120cm

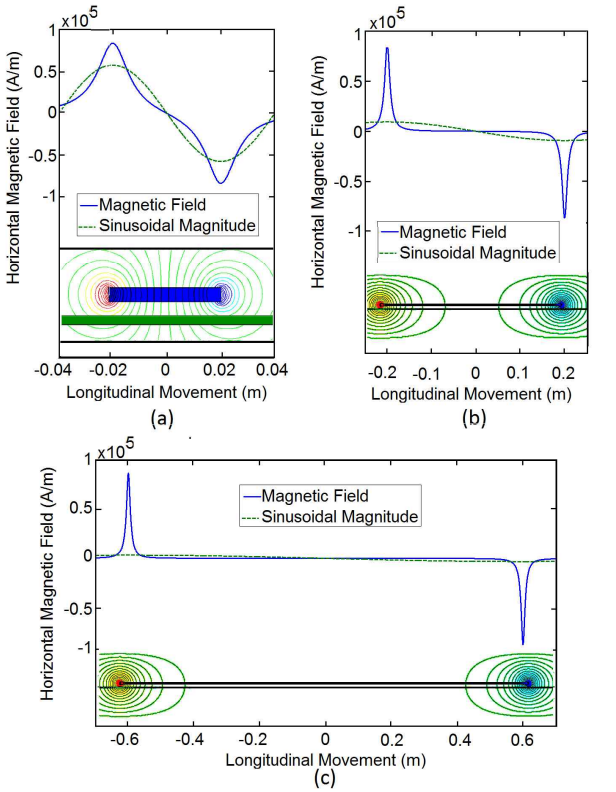

Fig. 5. Horizontal magnetic field diagram in different PM lengths (a) L=4cm (b) L=40cm (c) L=120cm

where the PM depth is sufficiently high. As a result, the reluctance of a possible path normal to the surface of Fig. 1 is very high and thus the flux in this direction is negligible and cannot contribute to the flux density in other directions.

Figs. 4 and 5 also show that a decreasing PM length reduces the effective spatial domain of the magnetic field. This leads to the reduction of the lift force. Therefore, it can be said that there is an optimum PM length for developing a maximum lift force. Solving the derivative of (14) with respect to PM length, an optimum PM length is obtained as:

$$\frac{\partial F_L}{\partial L}=0\longrightarrow L_{opt}=2\pi(y_0+\frac{D}{2}). \tag{16}$$

By substituting (16) into (14), the maximum lift force is obtained as:

$$F_{LMax.}=\frac{4\mu_0(M_0D)^2}{\pi^3 e(y_0+\frac{D}{2})}\cdot\frac{V_x{}^2}{V_x{}^2+w^2}. \tag{17}$$

According to (6), increasing the PM thickness leads to increase of the PM magnetomotive force and consecutively increase in the sinusoidal magnitude of the magnetic field. But again flux lines have to go through the closed paths with larger reluctances. Hence, it can be said that the developed lift force does not increase by the thickening of the PMs beyond a certain value. The variations of lift force per unit depth of the PM with respect to the PM dimensions at the velocity of 100m/s are shown in Fig. 4.

4. Optimization of PM Dimensions

In this study, the main target in obtaining the PM dimensions is achieving maximum lift force in a minimum material cost. The sensitivity analysis of the preceding section indicates that the PM dimensions cause conflict in meeting the mentioned target as it is elaborated below:

1. Increasing the PM dimensions does not always lead to increase in the lift force as a seen in Fig. 6.
2. Even though the lift force often increases with the PM thickness, the PM cost increases by increasing its thickness.

Therefore, for achieving the main target, the optimization is necessary to determine PM length and PM thickness. An objective optimization function for maximizing lift force while material cost of the PM EDS system in a general form can be formulated as:

$$J=\frac{F_L}{C}, \tag{18}$$

where C is the material cost and is defined as:

$$C = C_{Al} + C_{PM}, \tag{19}$$

where C_{Al} stands for aluminum conducting sheet cost and C_{PM} denotes neodymium magnet cost (both for a unit depth). A cylindrical aluminum body is used as a conducting sheet. By considering a cubic neodymium PM, C_{Al}, PM mass per unit depth (M_{PM}) and C_{PM} can be defined as:

$$C_{Al} = (\pi d_c d)\rho_{Al}\left(\frac{\$}{kg}\right)_{Al}, \tag{20}$$

$$M_{PM} = (LD)\rho_{NdFeB} \tag{21}$$

$$C_{PM} = M_{PM}\left(\frac{\$}{kg}\right)_{NdFeB}. \tag{22}$$

Obviously, maximizing of the objective function J will improve our objectives simultaneously. By using an aggregated objective function such as J, appropriate EDS system parameters can be selected. In this case, design parameters are PM length (L) and PM thickness (D). Also, some of the variables are assumed to be fixed, which are air-gap (y_0), PM magnetization (M_0), sheet conductivity (σ), sheet thickness (d), conducting sheet cylinder dimension (d_c), conducting sheet material density (ρ_{Al}), permanent magnet material density (ρ_{NdFeB}), conducting sheet cost per weight ($(\$/kg)_{Al}$), and permanent magnet cost per weight ($(\$/kg)_{NdFeB}$). The values for these variables are given in Table 1.

Table 1. Values of fixed variables of suspension system

Parameter	Unit	Value	Symbol
Air Gap	mm	5	y_0
PM Magnetization	A/m	838000	M_0
Sheet Conductivity	S/m	3.85×107	σ
Conducting Sheet Material	Kg/m3	2700	ρ_{Al}
Conducting Sheet Cylinder	m	0.5	Dc
Conducting Sheet Cost per	$/kg	1.82	$(\$/kg)_{Al}$
Permanent Magnet Material	Kg/m_3	7400	ρ_{PM}
Permanent Magnet Cost per	$/kg	60	$(\$/kg)_{PM}$

As an initial value for the solution, a permanent magnet of the size 45mm×5mm is selected. These dimensions are based on the experimental set-up and they are shown in Table 2 as original EDS parameters.

As mentioned in section II, it is assumed that the PM depth is large enough with respect to the PM thickness. This assumption is met in some real world applications and justifies the analytical derivation of lift and drag forces based on 2-D modeling. Thus, the PM thickness is to be limited by an upper value, in accordance to the assumption. However, in low PM thicknesses, the PM cannot close flux lines due to small amount of magnetomotive force. Therefore, the PM thickness must be constrained by a lower value as well. The PM length is limited by the upper and lower values around the original PM length. These constraints for design variables are listed in Table 2. Different design schemes are considered in this section depending on the selected objectives.

It is noted that the optimum point of PM length and PM thickness are independent from velocity and it can be applied in any arbitrary velocity that is based on the system steady speed. Genetic algorithm (GA) is employed to find the optimal design parameters. The selected GA parameters are shown in Table 3.

The variations of objective function with varying PM dimensions at 100 m/s velocity are shown in Fig. 7. For each value of PM thickness, an optimum PM length can be found; while, on the other hand increasing the PM

Table 2. Design parameters bounds

Parameter	Unit	Symbol	Min	Max	Original EDS
PM Length	mm	L	15	100	45
PM Thickness	mm	D	1	15	5

Table 3. Genetic algorithm parameters

Parameter	Value
Population Size	40
Probability of Crossover	0.8
Probability of Mutation	0.01
Number of Generations	400

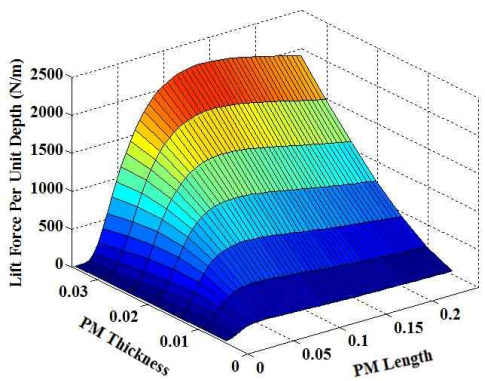

Fig. 6. Lift force per unit length with respect to PM dimensions in 100 m/s velocity

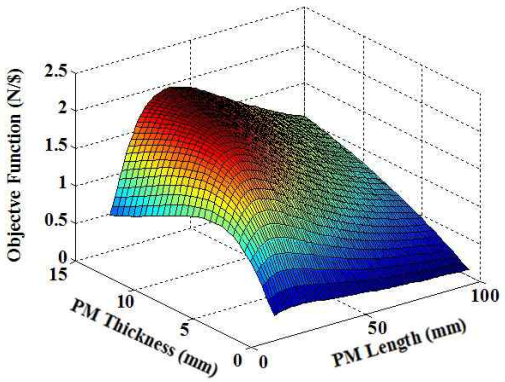

Fig. 7. Variations of lift force to the material cost ratio in terms of PM dimensions in 100m/s velocity

Table 4. Parameter of optimized and original EDS system

Parameter (Unit)		Optimized EDS system	Original EDS system
PM length (mm)		37	45
PM thickness (mm)		12.5	5
Lift (N)	Analytical	425	133.74
	FEM	436.4	134.7
Material cost ($)		203.35	115.34
F_L/C (N/$)		2.09	1.16
F_L/M_{PM} (N/Kg)		12.42	8.03

thickness, at the given acceptable range, can increase the overall value of the objective function. This optimum point yields the most efficient use of PM with maximum amount of developed lift force, which means that the scheme gives an optimum compromise between the smallest possible PM dimensions and a highest possible developed lift force. The parameters of optimized and original EDS system are listed in Table 4. These results show that the length of the PM reduces from 45 mm to 37 mm, while its thickness increases from 5 mm to 12.5 mm. Thickening PM leads to increase in the effective airgap (y_0+D/2). Also, the PM magnetomotive force is increased according to (6). All in all, the magnetic field and lift force is increased by thickening the PM as seen in Table 4.

The PM cross area increases from 2.25 cm^2 to 4.625 cm^2 in the optimized design. As so, the optimization leads to about 105% more PM consumption and mass. Also, the lift force increases more than three times from 133.74 N to 425 N as can be seen in the fourth row of Table 4. Therefore, the obtained specifications would provide a significantly higher lift force to material cost ratio which is 2.09 N/$ and lift force to PM mass which is 12.42 N/Kg compared to the previous ratio which were 1.16 N/$ and 8.03 N/Kg.

5. FEM and Experimental Validation

5.1 Finite element results

A 2-D FEM analysis is used to evaluate the PM EDS model in different PM dimensions. The network mesh of the model is shown in Fig. 8. It consists of two types of elements: the elements with 1 mm thickness at motion band and the elements with 5 mm thickness at other regions.

Variations of the lift and drag forces per unit of depth with respect to the length and thickness of neodymium PM at a velocity of 100 m/s are shown in Figs. 9 and 10 respectively. A good agreement between FEM and analytical results are seen. The discrepancy of the analytical and FEM results will increase if PM thickness increases with respect to PM length. This is because the modeling of PM by a single current sheet is not valid for high PM thicknesses with respect to the PM length [9]. The EDS

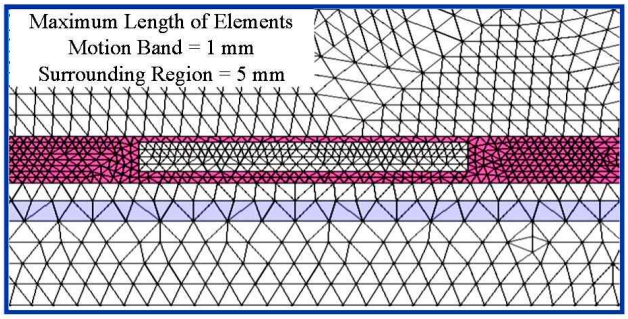

Fig. 8. Mesh generation of PM EDS model

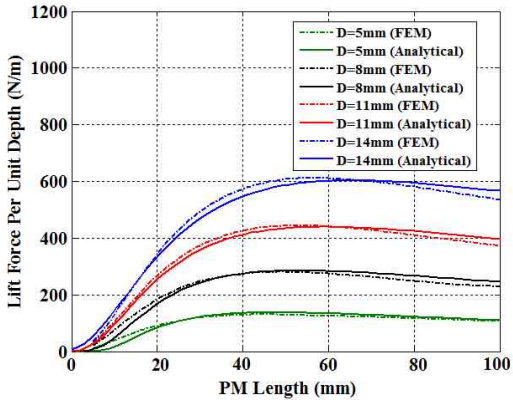

Fig. 9. Lift force per unit depth in terms of PM length in different thicknesses in 100 m/s velocity

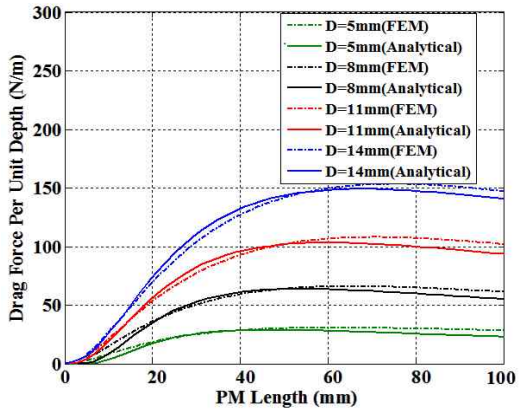

Fig. 10. Drag force per unit depth in terms of PM length in different thicknesses

systems obtained by the design optimization of section III are also evaluated by two dimensional finite element analysis. The lift and drag forces are calculated for different PM dimensions and sheet thicknesses obtained from the optimizations. It can be seen from Table 4 that there is a good agreement between the results of the FEM simulation and the ones produced by the proposed analytical model, since the discrepancy never exceeds 5%. Thus, validity of the model confirms the validity of the obtained results from the optimization.

5.2 Experimental validation

A Permanent magnet suspension system consisting of a PM block, an aluminum cylinder, and measuring devices is used for experimental evaluation. A schematic view of the experimental set-up is shown in Fig. 11. A three-phase supply is used to power a variable speed drive that rotates the aluminum cylinder. The rotational speed of the aluminum cylinder is measured by a tachometer and lift and drag forces are measured by loadcells. Also the air gap is determined by a sensor. The measuring devices then amplified by operational amplifiers and are sent to the computer via an interface board to be analyzed. A DC switching power supply provides a 12-V DC voltage for measuring devices and amplifiers.

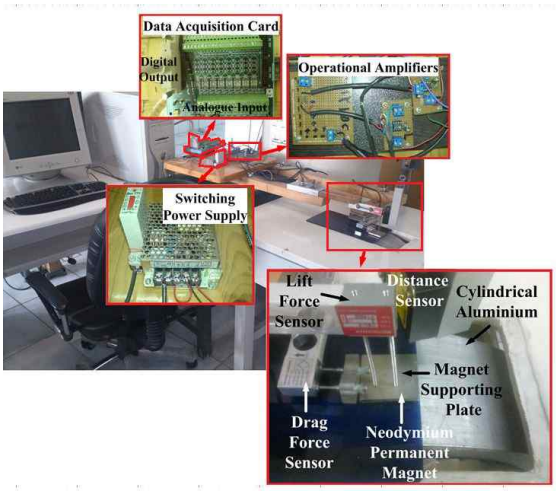

Fig. 11. Experimental PM EDS system

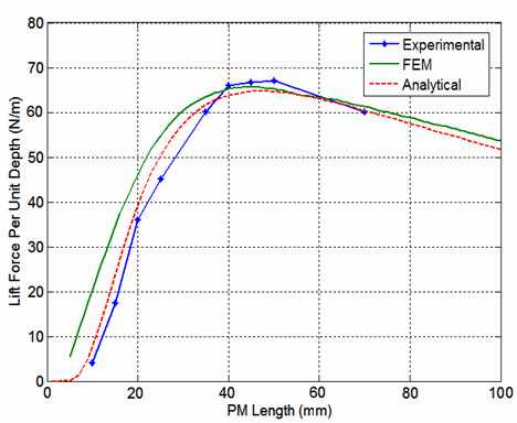

Fig. 12. FEM, analytical and experimental results of lift force per unit depth in 20m/s velocity

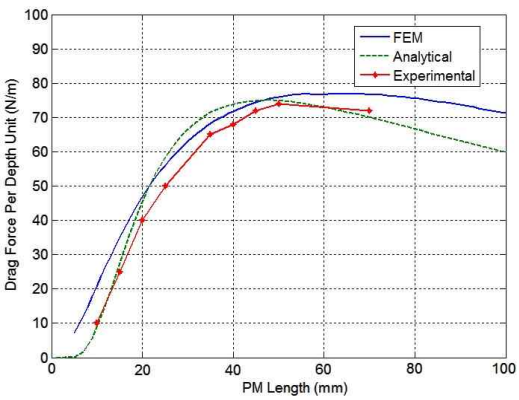

Fig. 13. FEM, analytical and experimental results of drag force per unit depth in 20m/s velocity

Analytical, FEM and experimental results of lift and drag forces in terms of PM length at a velocity of 20 m/s are shown in Figs. 12 and 13 respectively. These forces are also measured for PM with 1, 1.5, 2, 2.5, 3.5, 4, 4.5, 5 and 7 cm length and 5 mm thickness at the same velocity. Experimental results show that in 5 mm thickness, the optimum length of PM for developing a maximum lift force (for a unit depth) is between 3.5 and 4.5 cm. Also, the analytical results have good agreements with the FEM and the experimental results.

6. Conclusion

Optimization of the PM EDS system is aimed to achieve high lift force, and low material cost as the objectives. Using analytical calculation of lift force of a PM EDS system, the sensitivity of the forces with respect to system parameters is analyzed. The analysis reviles that the PM length and thickness can cause conflict in meeting the objective of maximum developed force and minimum material cost. Concerning these parameters, an optimization is proposed to meet the objectives. Genetic algorithm is used to carry out the optimization. Finally, the PM EDS model and the related optimization is validated by 2-D FEM and experimental results. The following analysis and design guidelines are obtained:

1. There is an optimum PM length for providing maximum sinusoidal magnetic field and lift force.
2. An optimum PM length for achieving maximum lift force can be obtained in terms of PM thickness.
3. The results show that substantial improvements in the ratio of the lift force to material cost is achievable simultaneously if optimal parameters are used.
4. Good agreement between analytical, FEM and experimental results confirms that 2-D analysis is accurate if the PM depth is much higher than PM thickness.

References

[1] R. F. Post, and D. D. Ryutov, "The Inductrack: a simpler approach to magnetic levitation," in *Applied Superconductivity, IEEE Transactions on*, vol. 10, no. 1, pp. 901-904, 2000.

[2] L. Xianxing, D. Jinyue, D. Yi, S. Kai, and M. Lihong, "Design and Static Performance Analysis of a Novel

Axial Hybrid Magnetic Bearing," *Magnetics, IEEE Transactions on,* vol. 50, pp. 1-4, 2014.
[3] F. Impinna, J. G. Detoni, N. Amati, and A. Tonoli, "Passive Magnetic Levitation of Rotors on Axial Electrodynamic Bearings," *Magnetics, IEEE Transactions on,* vol. 49, pp. 599-608, 2013.
[4] F. Safaei, A. A. Suratgar, A. Afshar, and M. Mirsalim, "Characteristics Optimization of the Maglev Train Hybrid Suspension System Using Genetic Algorithm," *Energy Conversion, IEEE Transactions on,* vol. PP, pp. 1-8, 2015.
[5] W. Kang, W. Dong, L. Heyun, S. Yang, Z. Xianbiao, and Y. Hui, "Analytical Modeling of Permanent Magnet Biased Axial Magnetic Bearing With Multiple Air Gaps," *Magnetics, IEEE Transactions on,* vol. 50, pp. 1-4, 2014.
[6] L. Xu and H. Bangcheng, "The Multiobjective Optimal Design of a Two-Degree-of-Freedom Hybrid Magnetic Bearing," *Magnetics*, *IEEE Transactions on,* vol. 50, pp. 1-14, 2014.
[7] B. Duck Kweon, C. Hungje, and L. Jongmin, "Characteristic Analysis of HTS Levitation Force With Various Conditions of Ground Conductors," *Applied Superconductivity, IEEE Transactions on,* vol. 18, pp. 803-807, 2008.
[8] L. Jongmin, B. Duck Kweon, K. Hyoungku, A. Min Cheol, L. Young-Shin, and K. Tae-Kuk, "Analysis on Ground Conductor Shape and Size Effect to Levitation Force in Static Type EDS Simulator," *Applied Superconductivity, IEEE Transactions on,* vol. 20, pp. 896-899, 2010.
[9] H. Rezaei and S. Vaez-Zadeh, "Modelling and analysis of permanent magnet electrodynamic suspension systems," *Progress In Electromagnetics Research M*, Vol. 36, 77-84, 2014.
[10] R. J. Hill, "Teaching electrodynamic levitation theory," *Education, IEEE Transactions on,* vol. 33, pp. 346-354, 1990.
[11] R. F. Post and D. D. Ryutov, "The Inductrack: a simpler approach to magnetic levitation," *Applied Superconductivity, IEEE Transactions on,* vol. 10, pp. 901-904, 2000.
[12] Business Insider. Markets Now. Available Online: http://markets.businessinsider.com/commodities/aluminum-price.
[13] European Commission. Materials Information System. Available Online: https://setis.ec.europa.eu/mis/ material/neodymium.

Saeed Hasanzadeh He received the B.S. degree from Shahroud University of Technology, Shahroud, Iran, in 2003, and the M.Sc. and Ph.D. degrees from University of Tehran, Tehran, Iran, in 2006 and 2012, respectively, all in electrical engineering. He joined the faculty of Electrical and Computer Engineering, Qom university of Technology as an Assistant Professor in 2013. His research interests include Power Electronics, Inductive Power Transfer Systems, Electrical Machines and Drives, Electric Vehicles, Magnetic Levitation Systems.

Hossein Rezaei He received the B.S. degree in Power and Water University of Technology, Tehran, Iran, in 2011, and the M.Sc. degree in University of Tehran, Tehran, Iran, in 2014. His main research interests include electrical machines design and analysis, modelling and optimization of magnetic suspension systems and hybrid and electrical vehicles.

Ehsan A. Qiyassi He received his B.Sc degree from Ferdowsi University of Mashhad and M.Sc. degree from University of Tehran in 2007 and 2014 respectively. He worked on high-power wireless power transfer for his master's thesis. He joined UMass Lowell in 2016 where he works on fault diagnosis of Doubly-Fed Induction Generators.